remote sensing

MDPI

Correction

Correction: Lanz et al. The InflateSAR Campaign: Developing Refugee Vessel Detection Capabilities with Polarimetric SAR. *Remote Sens.* 2023, *15*, 2008

Peter Lanz [1,2,*], Armando Marino [3], Morgan David Simpson [3], Thomas Brinkhoff [2], Frank Köster [1,4] and Matthias Möller [5]

1 Department of Computing Science, Carl von Ossietzky University of Oldenburg, Ammerländer Heerstraße 114-118, 26129 Oldenburg, Germany; frank.koester@dlr.de
2 Institute for Applied Photogrammetry and Geoinformatics, Jade University Oldenburg, Ofener Str. 16/19, 26121 Oldenburg, Germany; thomas.brinkhoff@jade-hs.de
3 Department of Biological and Environmental Sciences, University of Stirling, Stirling FK9 4LA, UK; armando.marino@stir.ac.uk (A.M.); m.d.simpson@stir.ac.uk (M.D.S.)
4 Institute for AI Safety and Security, German Aerospace Center (DLR), Rathausallee 12, 53757 Sankt Augustin, Germany
5 Faculty for Humanities and Cultural Sciences, Otto-Friedrich-University of Bamberg, Am Kranen, 96045 Bamberg, Germany; matthias.moeller@uni-bamberg.de
* Correspondence: peter.lanz@uni-oldenburg.de

Error in Figure

In the original publication [1], there was a mistake in the legend for Figures 11a–h, 12a–d and 13a–d. All 16 Figures have the headline "Incidence Angle" which is wrong and was removed in the corrected figures below. The correct Figures 11–13 appears below.

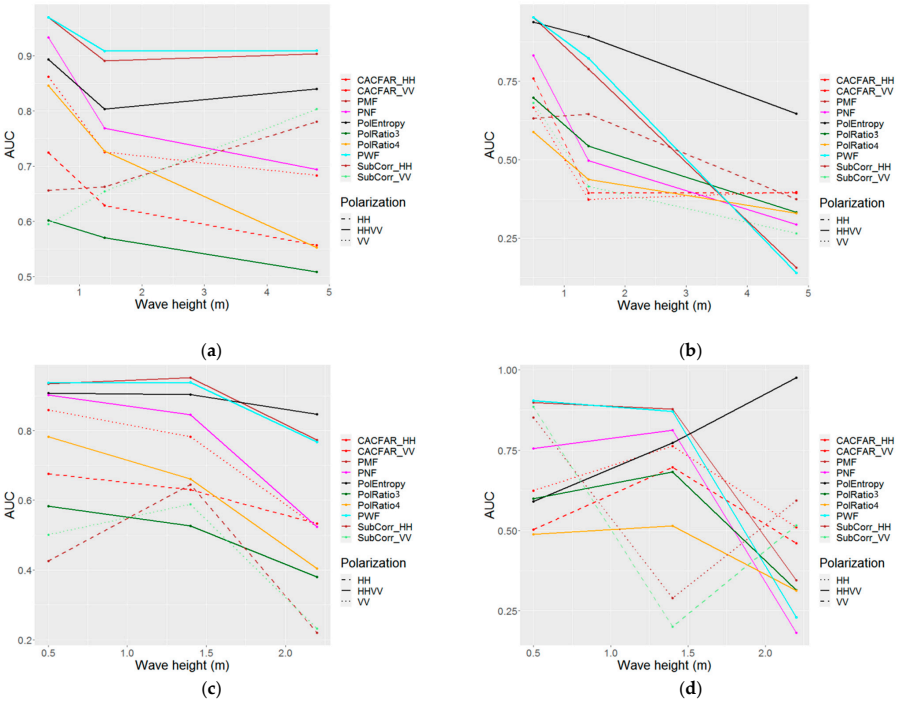

Figure 11. *Cont.*

check for updates

Citation: Lanz, P.; Marino, A.; Simpson, M.D.; Brinkhoff, T.; Köster, F.; Möller, M. Correction: Lanz et al. The InflateSAR Campaign: Developing Refugee Vessel Detection Capabilities with Polarimetric SAR. *Remote Sens.* 2023, *15*, 2008. *Remote Sens.* **2023**, *15*, 5344. https://doi.org/10.3390/rs15225344

Received: 26 June 2023
Accepted: 19 July 2023
Published: 13 November 2023

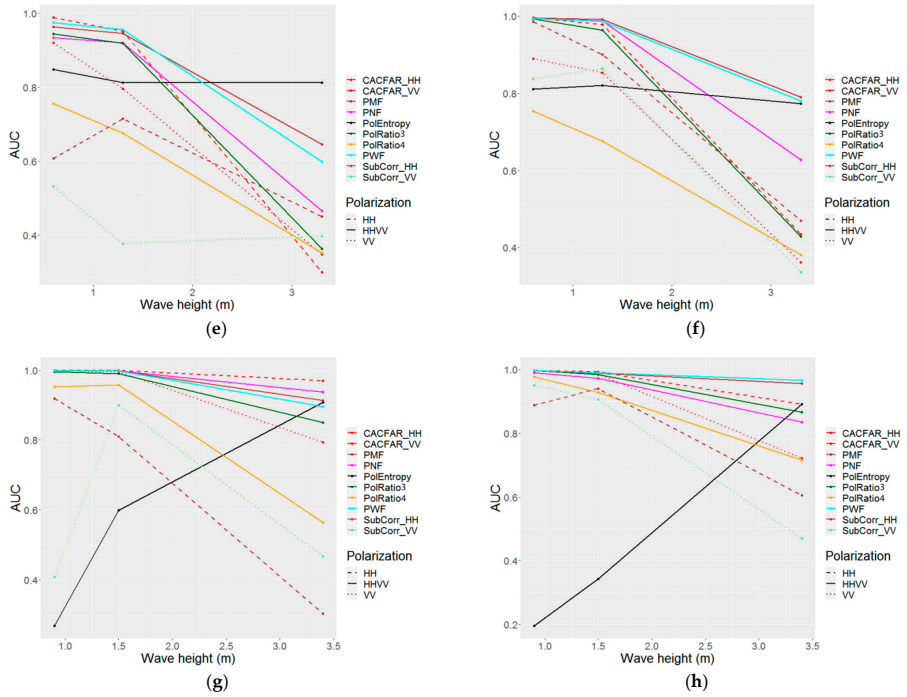

Figure 11. Comparison of the detector AUCs for different wave heights for HH VV. (**a**) Wind: cross, incidence angle: low and boat orientation: 45°. (**b**) Wind: cross, incidence angle: low and boat orientation: 90°. (**c**) Wind: up/down, incidence angle: low and boat orientation: 45°. (**d**) Wind: up/down, incidence angle: low and boat orientation: 90°. (**e**) Wind: up/down, incidence angle: medium and boat orientation: 45°. (**f**) Wind: up/down, incidence angle: medium and boat orientation: 90°. (**g**) Wind: up/down, incidence angle: high and boat orientation: 45°. (**h**) Wind: up/down, incidence angle: high and boat orientation: 90°.

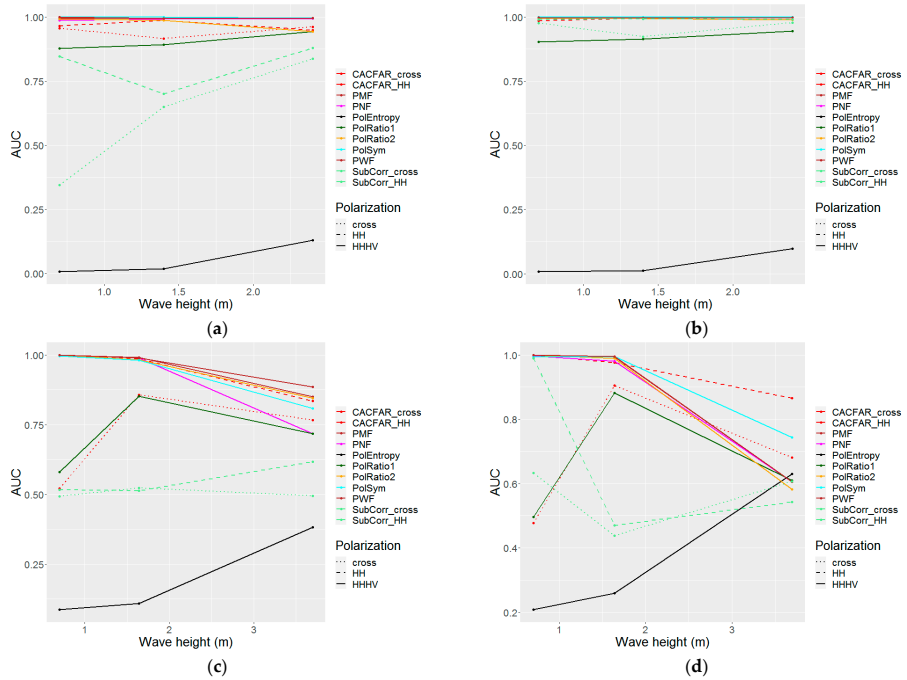

Figure 12. Comparison of the detector AUCs for different wave height for HV HH. (**a**) Wind: up/down, incidence angle: medium and boat orientation: 45°. (**b**) Wind: up/down, incidence angle: medium and boat orientation: 90°. (**c**) Wind: up/down, incidence angle: high and boat orientation: 45°. (**d**) Wind: up/down, incidence angle: high and boat orientation: 90°.

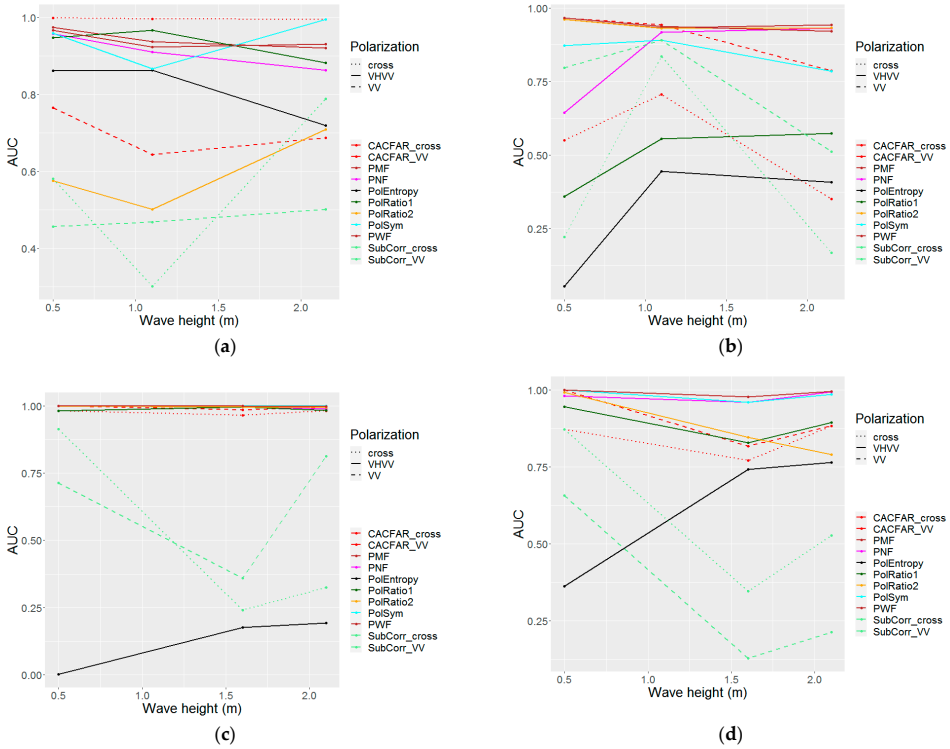

Figure 13. Comparison of the detector AUCs for different wave heights for VH VV. (**a**) Wind: up/down, incidence angle: medium and boat orientation: 45°. (**b**) Wind: up/down, incidence angle: medium and boat orientation: 90°. (**c**) Wind: up/down, incidence angle: high and boat orientation: 45°. (**d**) Wind: up/down, incidence angle: high and boat orientation: 90°.

Error in Table

In the original publication, there was a mistake in Tables 11–13 as published. The names of the detectors in row 5 ("PolRatio1") and in row 6 ("PolRatio2") are incomplete. The corrected Tables 11–13 appears below.

Table 11. The AUCs of the vessel-detection algorithms with different sensor parameters. The background colours indicate different AUCs from white (low AUCs) to dark green (very high AUCs).

Polarization		**HH VV**		**HV HH**		**VH VV**		
Incidence Angle	**Low**	**Medium**	**High**	**Medium**	**High**	**Medium**	**High**	**Avg**
PMF	0.787	0.888	0.976	0.996	0.906	0.945	0.995	**0.928**
PWF	0.779	0.882	0.975	0.997	0.912	0.941	0.995	**0.926**
PNF	0.67	0.822	0.956	0.994	0.881	0.871	0.986	**0.883**
PolEntropy	0.834	0.813	0.534	0.046	0.279	0.559	0.373	**0.491**
PolRatio1/3	0.529	0.768	0.947	0.913	0.689	0.714	0.939	**0.786**
PolRatio2/4	0.554	0.599	0.849	0.983	0.9	0.768	0.936	**0.799**
SubCorr_HH	0.565	0.688	0.744	0.9	0.608			**0.701**
SubCorr_VV	0.528	0.557	0.684			0.604	0.481	**0.571**
SubCorr_cross				0.785	0.531	0.483	0.537	**0.584**
CACFAR_HH	0.6	0.775	0.975	0.98	0.943			**0.854**
CACFAR_VV	0.628	0.695	0.915			0.798	0.946	**0.797**
CACFAR_cross				0.972	0.701	0.766	0.909	**0.837**
PolSym				0.999	0.92	0.895	0.991	**0.951**
avg	**0.647**	**0.749**	**0.856**	**0.869**	**0.752**	**0.759**	**0.826**	

Table 12. The AUCs of the vessel-detection algorithms with high sea states (SPAN > −17 dB). The background colours indicate different AUCs from white (low AUCs) to dark green (very high AUCs).

Polarization		**HH VV**			**HV HH**			**VH VV**	
Incidence Angle	**Low**	**Medium**	**High**	**Medium**	**High**	**Medium**	**High**	**Avg**
PMF	0.787	0.843	0.935		0.728	0.945		**0.848**
PWF	0.779	0.83	0.932		0.745	0.941		**0.846**
PNF	0.67	0.75	0.887		0.662	0.871		**0.768**
PolEntropy	0.834	0.804	0.9		0.506	0.559		**0.721**
PolRatio1/3	0.529	0.669	0.858		0.664	0.714		**0.687**
PolRatio2/4	0.554	0.521	0.64		0.714	0.768		**0.639**
SubCorr_HH	0.565	0.634	0.455		0.58			**0.558**
SubCorr_VV	0.528	0.494	0.468			0.604		**0.523**
SubCorr_cross					0.551	0.483		**0.517**
CACFAR_HH	0.6	0.666	0.931		0.85			**0.762**
CACFAR_VV	0.628	0.59	0.758			0.798		**0.694**
CACFAR_cross					0.723	0.766		**0.745**
PolSym					0.776	0.895		**0.835**
avg	**0.647**	**0.68**	**0.776**		**0.682**	**0.759**		

Table 13. The AUCs of the vessel-detection algorithms with different orientations of the rubber vessel. The blue background colours indicate better AUCs for the 45° inclined vessel, the orange colours show higher AUCs for the vessel oriented at 90°.

Polarization		**HH VV**			**HV HH**			**VH VV**	
Incidence Angle	**Low**	**Medium**	**High**	**Medium**	**High**	**Medium**	**High**	**Avg**
PMF	0.23	−0.07	−0.01	0	0.08	0	0.01	**0.03**
PWF	0.25	−0.08	−0.02	0	0.09	0	0.01	**0.04**
PNF	0.22	−0.10	0.05	−0.01	0.04	0.08	0.02	**0.04**
PolEntropy	0.06	0.02	0.12	0.01	−0.17	0.51	−0.50	**0.01**
PolRatio1/3	0	−0.05	0	−0.02	0.05	0.44	0.1	**0.07**
PolRatio2/4	0.22	−0.01	−0.05	−0.02	0.09	−0.35	0.12	**0**
SubCorr_HH	0	−0.19	−0.13	−0.18	−0.12			**−0.13**
SubCorr_VV	0.07	−0.24	−0.18			−0.26	0.3	**−0.06**
SubCorr_cross				−0.35	−0.06	0.15	−0.09	**−0.09**
CACFAR_HH	0.05	−0.06	0.03	−0.03	−0.01			**0**
CACFAR_VV	0.22	−0.01	0.03			−0.20	0.09	**0.03**
CACFAR_cross				−0.06	0.03	0.46	0.14	**0.14**
PolSym				0	0.02	0.09	0.02	**0.03**
avg	**0.13**	**−0.08**	**−0.02**	**−0.06**	**0**	**0.08**	**0.02**	**0.01**

The authors state that the scientific conclusions are unaffected. This correction was approved by the Academic Editor. The original publication has also been updated.

Reference

1. Lanz, P.; Marino, A.; Simpson, M.D.; Brinkhoff, T.; Köster, F.; Möller, M. The InflateSAR Campaign: Developing Refugee Vessel Detection Capabilities with Polarimetric SAR. *Remote Sens.* **2023**, *15*, 2008. [CrossRef]